

Astrophysical Journal – submitted: 2004 March 5; accepted:
2004 August 3

Studying The Star Formation Histories of Galaxies in Clusters from Composite Spectra

Alan Dressler & Augustus Oemler, Jr.

Carnegie Observatories, 813 Santa Barbara St., Pasadena, California 91101-1292

dressler@ociw.edu, oemler@ociw.edu

Bianca M. Poggianti

Osservatorio Astronomico di Padova, vicolo dell'Osservatorio 5, 35122 Padova, Italy

poggianti@pd.astro.it

Ian Smail

Department of Physics, University of Durham, South Rd, Durham DH1 3LE, UK

Ian.Smail@durham.ac.uk

Scott Trager

*Kapteyn Institute, Rijksuniversiteit Groningen, Postbus 800, NL-9700 AV Groningen,
Netherlands*

sctrager@astro.rug.nl

Stephen A. Sheckman

Carnegie Observatories, 813 Santa Barbara St., Pasadena, California 91101-1292

shec@ociw.edu

Warrick J. Couch

*School of Physics, University of New South Wales, Sydney 2052, Australia,
w.couch@unsw.edu.au*

Richard S. Ellis

California Institute of Technology, Pasadena, California, rse@astro.caltech.edu

ABSTRACT

We have formed “composite spectra” by combining the integrated–light spectra of individual galaxies in 8 intermediate–redshift and 12 low–redshift clusters of galaxies. Because these composite spectra have much higher signal–to–noise ratios than individual galaxy spectra, they are particularly useful in quantifying general trends in star formation for galaxy populations in distant clusters, $z > 0.3$. By measuring diagnostic features that represent stellar populations of very different ages, a grand–composite spectrum can reflect the fractions of those populations as accurately as if excellent spectral measurements were available for each galaxy. Such composite spectra can also be useful in the study of finer spectral signatures, for example, spectral indices that break the age–metallicity degeneracy, and the shape of the $H\delta$ absorption line as an indicator of the age and duration of an epoch of starbursting galaxies in a cluster.

Measuring the equivalent widths of spectral features in composite spectra is especially well–suited for comparing cosmic variance of star formation in clusters at a given redshift, or comparing clusters over a range of redshifts. When we do this we find that [O II] emission and especially Balmer absorption is strong in each of our intermediate–redshift clusters, and completely separable from a sample of 12 *present–epoch* clusters, where these features are weak. Cluster–to–cluster variations at a given epoch seem to be smaller than the strong trend in redshift, which suggests that cosmic evolution is the major factor in the star formation histories of cluster galaxies. Specifically, we show by comparing to the $H\delta$ strengths of present–epoch populations of continuously star–forming galaxies that the higher–redshift samples must contain a much higher fraction of starburst galaxies than are found today in any environment.

Subject headings: galaxies: clusters: general — galaxies: evolution

1. Introduction

Butcher and Oemler’s (1978a,b) report of strong color evolution of cluster galaxies since $z = 0.5$ was unexpected within the context of ideas about galaxy evolution that were prevalent at the time. Studies of the stellar populations of nearby galaxies had fostered the notion that elliptical and S0 galaxies are basically old stellar systems; the population of present–epoch clusters are so dominated by these types that it seemed surprising that rich clusters would have been sites of significant star formation only ~ 4 Gyr ago. Nevertheless,

the blue colors Butcher & Oemler observed for one-third to one-half the galaxies in the original two clusters of their study suggested just that. At that time, before hierarchical clustering became the popular paradigm for galaxy evolution, the idea that these early type galaxies might be assembled so recently — scarcely one-third of a Hubble time ago — was a radical proposition.

In the following two decades, evidence for the Butcher–Oemler effect accumulated (see, e.g., Margoniner & de Carvalho 2000, Margoniner et al. 2001) and the focus began to shift to spectroscopic studies which could connect the Butcher–Oemler effect with the individual and collective evolution of star forming galaxies in the cluster environment. Dressler & Gunn (1982, 1983) were the first to confirm that the blue populations of the Butcher–Oemler clusters were the result of star formation, and also to point out that the presence of strong H δ absorption indicated a greater prevalence of starburst galaxies than are found today (Couch & Sharples 1987; Giraud 1990; Kelson et al. 1997, 2000; Tran et al. 2003). Our present collaboration — the Morphs — has obtained a large spectroscopic sample and presented evidence for a strong spectral evolution of galaxies in rich clusters since $z \sim 0.5$. Our technique has been to use the spectral features of individual galaxies to assign them different spectral classes (Dressler et al. 1999, D99; Poggianti et al. 1999, P99), and compare clusters using their fractions of the different spectral classes. For our ten-cluster intermediate-redshift sample, P99 used this approach to conclude that, within counting statistics, all exhibit the same behavior of enhanced ongoing star formation compared to present-epoch clusters, and a much pronounced component of starburst galaxies. However, other studies have reported on clusters that appear to have much less ongoing or recent star formation, in particular, much less in the form of starbursts (Balogh et al. 1999). The attempt to resolve whether this is a genuine difference of cluster populations has made clear that the barely adequate signal-to-noise ratio (S/N) of the spectra in these studies, and the lack of agreement on a common system of spectral classes, hampers efforts to arrive at a consistent picture.

We present here a new technique of comparing clusters or any galaxy populations that facilitates such comparisons, based on coadding all available spectra in each cluster. The idea is to obtain a composite of the starlight over the cluster, by adding spectra of *a representative population of galaxies in the cluster*. For a sample of clusters, if the available spectra sample the galaxy population to a similar magnitude limit and magnitude distribution, and are unbiased with respect to color or type, co-adding a sufficient number of spectra will produce for each cluster a high S/N spectrum of the composite stellar population. In these composite spectra the absorption and emission features that are used to assess star formation history are very well defined, so the comparison between clusters, and between studies, should be much easier to make, and more reliable.

For this study we have chosen to measure [O II] emission and H δ absorption in the composite spectra. By this choice we are essentially asking: (1) How much of the light in the cluster is “old” — more than a few Gyr? (2) How much has an age 500 Myr to 1 Gyr — the lifetimes of A-stars? (3) How much is from active regions of star formation with characteristic ages of 10^7 years? Because these three populations are temporally distinct, they provide a sort of orthonormal basis set for dissecting the population of a single galaxy or an entire cluster, and, since composite spectra have a high S/N ratio compared to the typical individual spectra, the results of such measurements are robust and unambiguous. They furthermore offer the potential of measuring more subtle features that are important diagnostics of stellar population evolution.

In P99 we analyzed spectra of individual cluster galaxies with strong [O II] and H δ and showed, by comparing to the models of continuously star-forming galaxies, that in numerous cases the strength of these features were the clear signature a starburst, or post-starburst star formation history. This result suggests an important change in the mode of star formation in dense environments over the last few billion years. Here, we will show that strong [O II] emission and H δ absorption is a prominent, perhaps universal, feature of the *composite* galaxy populations of $z \sim 0.5$ clusters, unlike their present-epoch counterparts. While the individual spectra of galaxies may tell us more about the mechanisms that are at work, or the range of behavior that is present, these composite measurements are a powerful tool in demonstrating the importance of pure time evolution of cluster populations versus cosmic variance that may relate to the dynamical history of individual clusters.

The paper is organized as follows: In §2 we describe the cluster samples and in §3 we describe the data used in this paper and the method of co-adding spectra in clusters and the field from $z = 0.03$ to $z = 0.91$. In §4 we discuss the results of comparing intermediate- and low-redshift clusters by means of their composite spectra, and the potential for using such high S/N spectra to answer more detailed questions about the stellar populations and the history of star formation. In §5, we focus on using H δ as a proxy for intermediate-age stellar populations. Specifically, we use the measurements of the equivalent widths (EW) of H δ in the composite spectra to discuss possibly disparate results found for the Morphs sample compared to those published for CNOC1 clusters. In §6 we summarize our results.

2. Cluster samples

Table 1 lists the clusters and the field samples for which we have performed the coaddition of spectra. There are eight clusters from the Morphs intermediate-redshift cluster

sample (D99),¹ supplemented by new data for A851 (Oemler et al. 2004), and an extensive sample of low-redshift clusters studied by Dressler & Shectman (1988, hereinafter DS). The number of coadded spectra for each group is listed in Table 1.

These two samples compare well in terms of luminosity depth; generally, the cluster samples are magnitude-limited and unbiased by type or color. Both are complete, in the sense that the spectroscopic samples follow the Schechter luminosity distribution down to the same absolute magnitude $M_V \sim -19.5$ (see, e.g., Fig. 6a of D99), although the low- z sample is more densely sampled by factors of 2–3. The completeness of each sample falls rapidly for fainter galaxies; the small number that are included contribute less than 10% of the total light. With respect to area (or volume), the DS sample clusters were studied within a radius of $R \sim 2$ Mpc,² while the Morphs clusters have been studied over a somewhat smaller $R \sim 1.5$ Mpc radius. This is a small difference compared to the core radii, which at any rate might be expected to result in an undersampling of star-forming galaxies in the distant clusters.

All of the Morphs clusters are rich, as confirmed by our spectroscopy and the large number of *bona fide* cluster members. None of them is contaminated by other significant structures along the line of sight (see Fig. 2 in D99), a common motivation for choosing clusters by X-ray luminosity. Interestingly, the Morphs clusters span a wide range in X-ray and optical properties (e.g. Smail et al. 1997). The structural properties of these clusters are diverse, including both regular, very concentrated clusters and irregular ones with clear substructure, such as Abell 851. Two of the Morphs clusters, CL0016+1609 and 3C295, are very luminous ($L_X \sim 12 \times 10^{44}$ and $L_X \sim 6.4 \times 10^{44}$ ergs s⁻¹, in the 0.3–3.5 keV range). For comparison, Coma has an X-ray luminosity intermediate between these two. The other Morphs clusters have progressively lower X-ray fluxes; overall they span a factor of 17 in X-ray luminosity. Abell 851, a rich but highly substructured cluster (Oemler et al. 2004), has $L_X \sim 2 \times 10^{44}$ ergs s⁻¹ (see also De Filippis, Schindler, & Castillo-Morales 2003). (These X-ray luminosities are from heterogeneous sources, as described in Smail et al. Section 2; here we are concerned only with an approximate ordering and range.)

The DS sample of nearby clusters spans an even larger range in X-ray luminosities than the Morphs sample (a factor ~ 24 in L_X). Abell 754 has an X-ray luminosity comparable to the brightest Morphs cluster, CL0016+1609, but overall, the low-redshift sample con-

¹The two southern clusters studied at the NTT, CL0054 and CL0412 of the D99 study, were not used because they contain a high fraction of spectra with poor sky subtraction.

²We adopt a standard Λ cosmology with a Hubble constant $H_o = 70$ km s⁻¹Mpc⁻¹ throughout this paper.

tains more lower mass, lower X-ray luminosity clusters than the Morphs sample (Ebeling et al. 1996, Girardi et al. 1998).

In order to get some indication of behavior at even higher redshift we have used data from an unpublished study of four clusters $0.65 < z < 0.76$ by Dressler and Gunn (referred to as DGhiz) — this sample is less deep in terms of absolute magnitude and less uniformly sampled. The DGhiz sample consists of 60 cluster members in CL0020+0407 ($z = 0.697$), CL0231+0032 ($z = 0.740$), CL1322+3027 ($z = 0.757$), CL1322+3114 ($z = 0.696$) from the Gunn, Hoessel, & Oke (1986) catalog. Data for another such cluster, MS1054 at $z = 0.83$, has been generously contributed by van Dokkum and collaborators. These higher redshift samples are used for illustrative purposes only and no conclusions in this study are based on them.

3. Spectral data and technique

The DS spectra were sampled with 2×4 arcsec apertures, a considerably smaller physical scale ($\sim 2 \times 4$ kpc) than the 1.5 arcsec slits with typical length of 3.0 arcsec ($\sim 9 \times 18$ kpc) used in the Morphs study. This difference is exaggerated since the light is more concentrated than these latter dimensions would suggest, nevertheless, this mismatch is potentially a matter of concern. The situation of robust star formation surrounding a very old bulge component is quite rare in present-epoch galaxies (and perhaps at higher redshift as well), and early-types rarely have strong population gradients of any kind, nevertheless, this is one area where a better match in the sampling could and should be made. The sense of the bias here would be to underestimate star formation in the present-epoch clusters.

Each of these studies has generated a *field* sample as well. The DS field sample ($z < 0.06$) is as representative as the DS cluster sample, but the Morphs field sample ($0.35 < z < 0.6$) is likely to be more heterogeneous than the Morphs cluster sample because of the way the wide redshift range plays off against the luminosity function. Although this is not a serious problem for this paper, it means that any conclusions based on a comparison of cluster and field at a given redshift are tentative. More complete field surveys and additional cluster samples do exist; they would be welcome additions to these analyses.

The DGhiz study adds another intermediate-redshift field sample which should be comparable in quality to the Morphs field sample, as well as a higher- z ($0.65 < z < 0.95$) field sample which is considerably smaller and almost certainly subject to serious selection effects. We judge the latter to be too ill-defined to be used in the present study.

We have excluded identifiable AGNs from our sums, using the criteria of D99, which

amounted to 1 DS galaxy, 7 in the Morphs cluster and field galaxies, but no DGhiz galaxies. For the Morphs cluster sample we have chosen only spectra of quality 1–3 (see D99); we have used any and all spectra from the DS study (all of which have high S/N compared to the distant sample) and all spectra with measured redshifts (60 cluster members) from the DGhiz sample.

Ideally, one would combine all the light from all galaxies to form a luminosity-weighted composite spectrum. Of course, this is impossible from the start because slit spectroscopy samples only a portion of the light in each galaxy. As an alternative, *for the cluster samples* we have normalized each spectrum to unity over the interval 4200–4600Å (approximating the rest-frame R-band but avoiding the Balmer absorption and [O II] emission) and weighted its contribution by the R-band galaxy luminosity, (The field samples are sufficiently inhomogeneous that we don’t consider such a weighting to be useful.) That is, we have assumed that each spectrum has sampled a representative piece of that galaxy’s stellar population (as also assumed in previous galaxy-by-galaxy analyses). Examples of the results of the summing procedure is shown in Figure 1, which presents the composite spectra in the [O II] to H δ wavelength range for 5 of the Morphs clusters and 5 of the DS low-redshift sample. The high S/N of these composite spectra — typically 5–10 times that of individual spectra (see Dressler et al. 1997) — is apparent. The MS1054 composite spectrum, kindly provided by P. van Dokkum, is spectral-flux-weighted sum (through the slit) of 72 I-selected cluster members (see van Dokkum et al. 2000).

As we have done for the individual Morphs spectra, we restrict ourselves in this study to measuring two spectral features. We use the strength of [O II] emission as an indicator of recent star formation; H α would be preferable, but this is not generally covered by the spectra. To isolate the intermediate-age population associated with starbursts or decaying star formation we use H δ absorption, whose properties are discussed in more detail in P99. H δ is a reliable indicator because it is the strongest of the Balmer lines for which there is minimal contamination by emission. $H\gamma$ and $H\beta$ lines are intrinsically stronger, but are more filled in by emission in galaxies with strong star formation (see, e.g., Trager et al. 2000a,b; Trager 2004). The higher order Balmer lines are even less subject to filling, but they are weaker and in less clean regions of the spectrum. The shape of the continuum around H δ is also the cleanest of any of the higher-order lines, being mostly devoid of strong nearby features, although it is not without difficulties, as discussed below.

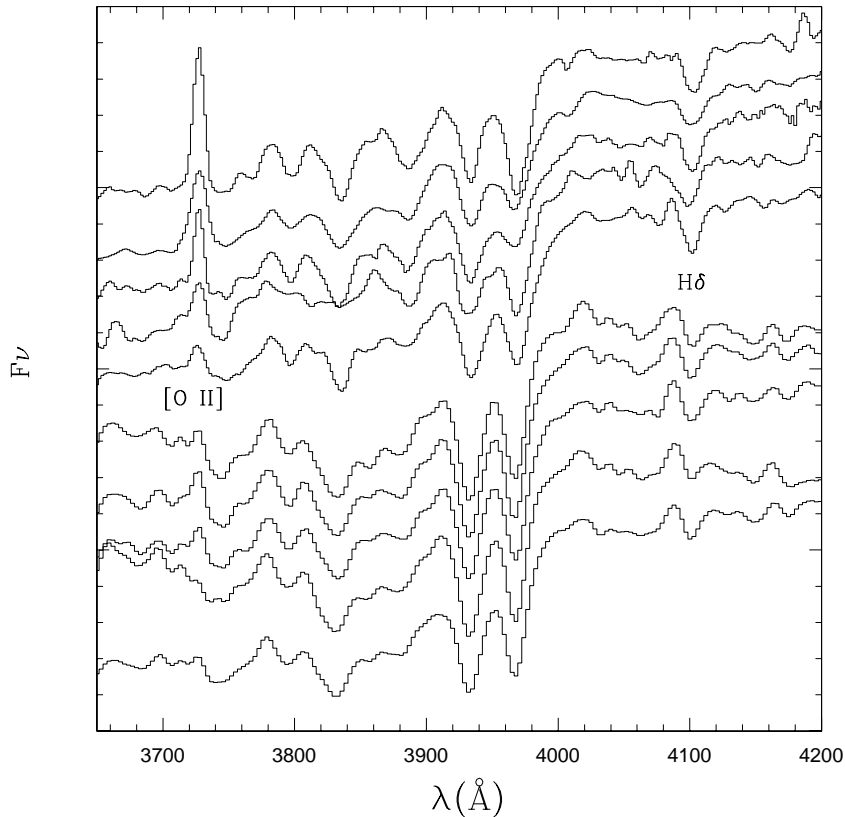


Fig. 1. Composite spectra for 5 intermediate-redshift clusters (above) and 5 low-redshift clusters (below) from the Morphs and DS samples. We have chosen the better examples, but [O II] and H δ are seen in all clusters of both samples; values for all clusters are tabulated and included in subsequent plots. The [O II] and H δ features are clearly stronger in the spectra of the intermediate-redshift clusters. Also apparent is the stronger contribution in the low-redshift cluster spectra of various lines around H δ that depress the continuum and leave what appears to be a peak immediately to the blue of H δ , as described in Section 4.2. On this and in the following plots, the ordinate $F\nu$ in $\text{ergs s}^{-1} \text{hz}^{-1}$ is in relative units.

The DS data have a spectral resolution of $\text{FWHM} \sim 5\text{\AA}$, while the Morphs spectra have a lower resolution of $\text{FWHM} \sim 9\text{\AA}$, in the rest frame. In order to correct for this difference, the DS data were smoothed by a Gaussian kernel to lower their spectral resolution to $\sim 9\text{\AA}$ FWHM. Also, to approximately match the 2.8\AA per pixel binning (rest frame) of the Morphs spectra, the DS data were rebinned to 3.0\AA per pixel. We found no strong sensitivity of our measurements to such adjustments, but differences were measured at the 10–20% level, primarily for H δ , which tends to drop in equivalent width with lower spectral resolution. Likewise, there should be a tendency to underestimate H δ strengths for galaxies with lower velocity dispersion, $\sigma < 150 \text{ km s}^{-1}$ in the DS spectra and $\sigma < 200 \text{ km s}^{-1}$ in the Morphs spectra. This suggests that the effect, if significant, goes in the direction of diluting the true strengths of H δ lines in the distant sample.

The measurement of [O II] emission is straightforward as this feature is unresolved in our data and found on a nearly-flat continuum. We use a line-fitting technique, as described in D99, however, a bandpass technique (subtracting the level of a band containing the feature from the average of two straddling continuum bands) would give as good a result for [O II]. The line-fitting technique is preferred for H δ because, as we discussed in Section 4.2, the line width and the character of the surrounding continuum change with the strength of the feature and the character of the stellar “background,” which itself seems to change with redshift. The high S/N of the composite spectra guarantees excellent fits to both H δ and [O II], with typical errors in equivalent width of less 10%.

4. Comparing clusters through composite spectra

The measured line strengths, EW([O II]) and EW(H δ) are given in Table 1. The results of this first attempt to study composite cluster populations, shown in Figure 2, are remarkably clear. The intermediate-redshift clusters all average H δ strengths of $\sim 2.0\text{\AA}$ and have substantial [O II] emission varying between -3\AA and -10\AA equivalent width; both are indicative of substantial ongoing star formation. In contrast, each of the low-redshift clusters shows much weaker EW(H δ) $\sim 1.3\text{\AA}$ — this is not just 35% weaker, but typical of a population that has had *no significant star formation* for several Gyr — and much weaker EW([O II]) = -2\AA to -5\AA . This difference in spectral characteristics, in particular, the appearance of many systems with strong Balmer lines in intermediate-redshift cluster samples noted by Dressler & Gunn (1983, see also Couch & Sharples 1987), appears to be primarily dependent on epoch. There may be some real sensitivity to cluster properties buried in the scatter in Figure 2, but much more data on each cluster will be needed to be certain that these are not just statistical errors.

It is interesting to note that, unlike the strong evolution in these features from low to intermediate redshift, there is no further significant increase for the even higher-redshift DG sample or for MS1054-03 at $z = 0.83$ (derived from data kindly provided P. van Dokkum). These clusters have composite values of EW(H δ) and EW([O II]) that are consistent within the errors with the Morphs intermediate-redshift sample. Although these first indications suggest that EW(H δ) and EW([O II]) do not continue to increase at higher redshift, it is clearly too early to tell. A particular concern is that the higher redshift clusters are not sampled as deeply, which means that fainter galaxies, which are by-in-large more likely to be the places of higher rates of star formation, comprise a smaller fraction of the sample.

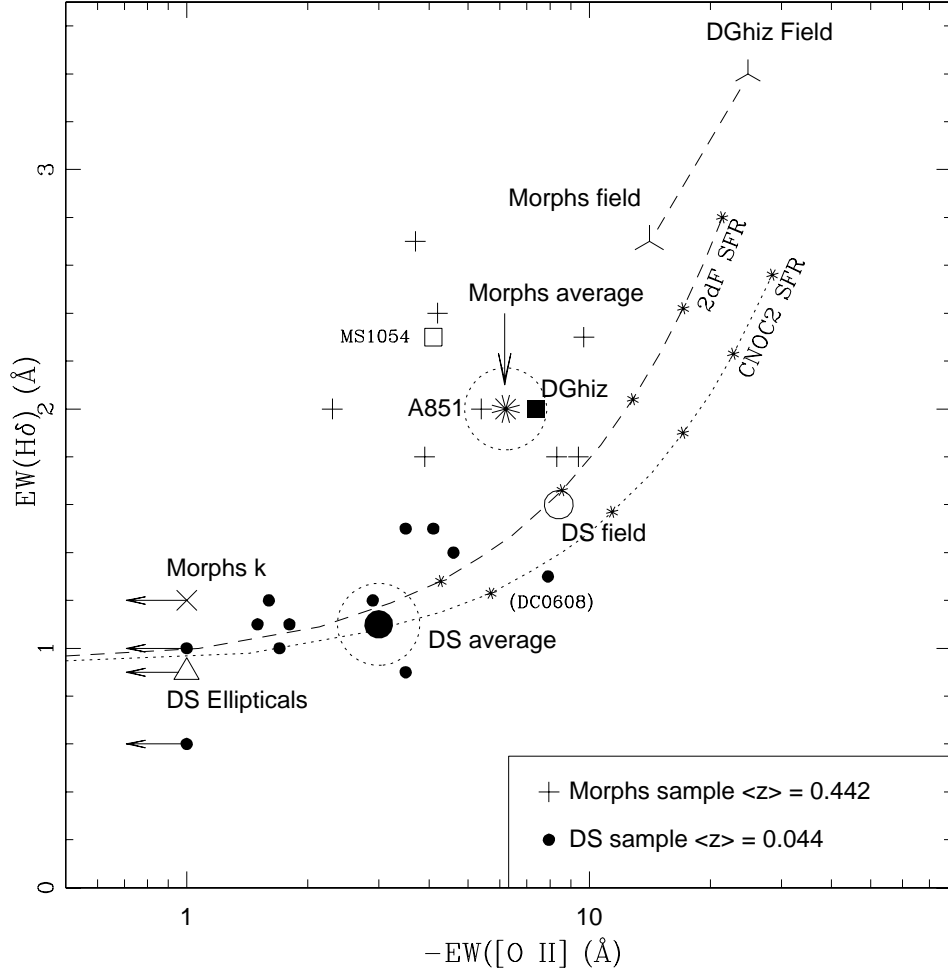


Fig. 2. Measurements of $EW([O II])$ and $EW(H\delta)$ for the various field and cluster samples of Table 1. There is a clear separation of the “mean” values of $H\delta$ for the Morphs and the DS samples, but there is also no overlap in the individual measurements for the clusters studied. Even higher-redshift clusters may share the properties of the Morphs sample, with no obvious further increase in activity from $z \sim 0.5$ to $z \sim 0.8$. As discussed in §4.1, the two lines represent different mixes of passive galaxies and continuously star-forming galaxies with $[O II]$ distributions from the 2dF Survey (dashed line) and the CNOC survey (dotted line). The small asterisks along the curve mark the appropriate values of $EW([O II])$ and $EW(H\delta)$ for 20%, 40%, 60%, 80%, and 100% mix of galaxies undergoing continuous star formation. Although such mixes adequately describe the low-redshift DS clusters and field, they fail to match any of the higher-redshift cluster or field samples, indicating the importance of starbursts to these galaxy populations.

Just as interesting and much more certain is the lack of overlap in the composite $H\delta$ strengths for the two primary samples: although the $[O II]$ strengths overlap considerably, there are no present-epoch clusters with strong $H\delta$ and no intermediate-redshift clusters in which it is weak. As we discuss below, there is the suggestion by Balogh et al. (1999) and Ellingson et al. (2001) that strong X-ray-emitting clusters at intermediate redshifts show less star formation activity than the Morphs clusters, but the spectroscopic data presented

here certainly offer no examples of the inverse, that is, present–epoch clusters resembling those of the Morphs sample. The universality of the result in Figure 2 must await further data from other clusters, but there seems little doubt that clusters with strong H δ absorption in their composite spectra are common at $z \sim 0.5$, and at best rare today.

In as much as the composite spectra of the 8 individual Morphs clusters are very similar, we produce the sum of the galaxies in *all* 8 clusters in Figure 3 (also plotted as a point in Figure 2). By subdividing this grand–composite spectrum into the Morphs spectral classes (described in D99), we create a recipe for a $z \sim 0.5$ cluster, shown in Figure 3 as the percentages of each type of spectrum that make up the whole. Even though $\sim 70\%$ of the galaxies do not have strong Balmer lines (primarily k and e(c) types) the signature of the H δ line is obvious in the composite spectrum — this shows how strong is the contribution of H δ from the remaining $\sim 30\%$, a fact that we attribute largely to starbursts, as we discuss in the next section.

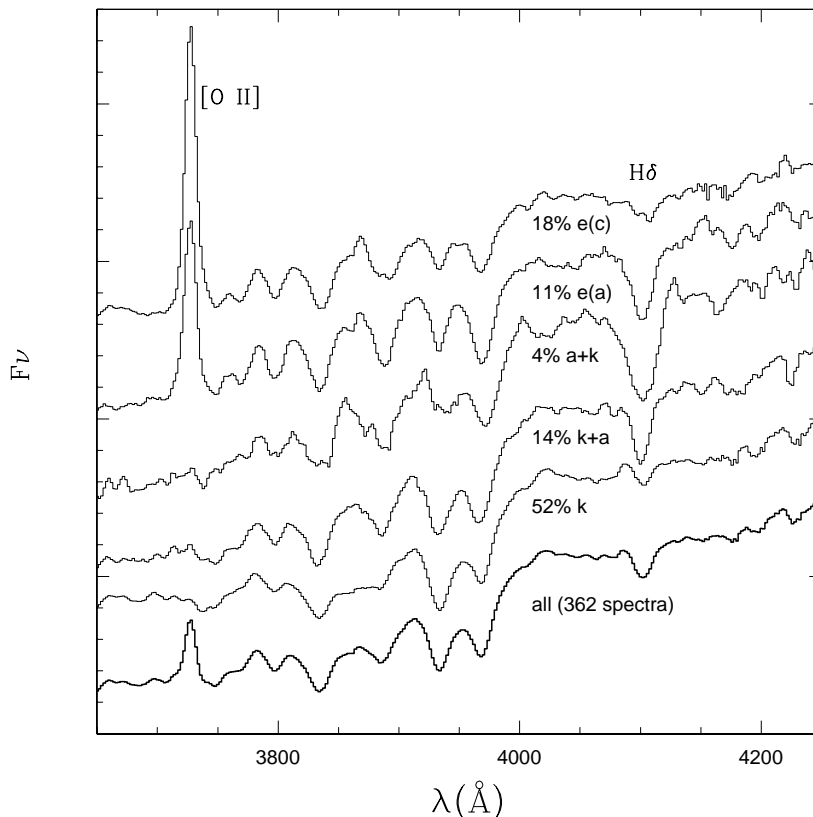


Fig. 3. The grand composite spectrum for galaxies in all 8 clusters at $z \sim 0.5$, excluding 7 AGN’s and 10 others with poor sky subtraction. The contribution to the combined spectrum (bottom) of [O II] and H δ from the “active” galaxies, k+a,

a+k, and e(a), is clearly seen. The fraction of each type is noted.

The comparison with field samples is also interesting. As has been found in other field surveys, the field at intermediate–redshift shows a considerably stronger [O II] than at $z \sim 0$, indicating a higher rate of star formation in the relatively recent past (e.g., Broadhurst, Ellis, & Shanks 1988). Not previously demonstrated, however, is the significantly greater strength of H δ in field galaxies at $z \sim 0.5$ and $z \sim 0.75$. Our two field samples at $z \sim 0.5$, from the Morphs study and the DGhiz sample, both exhibit a much stronger H δ absorption than the low–redshift DS field. The obvious question is, for both cluster and field, do these stronger H δ lines represent simply a higher fraction of galaxies with strong, continuous star formation, or do they also point to a significant increase in the fraction of starburst galaxies in the field? To answer this question, we must compare to the expected strength of H δ for populations of galaxies undergoing continuous star formation.

4.1. Expectations for continuously star–forming galaxies

In this section we determine the mean values of EW([O II]) and EW(H δ) that are expected for different mixes of passive galaxies and continuously star forming galaxies. Our goal is to test whether any such populations, regardless of proportions, are able to account for the locus of points we find for the intermediate–redshift clusters and field.

It might be possible to calculate the expected mean values of EW([O II]) vs EW(H δ) using stellar population models, but we prefer to stick as closely as possible to empirical data. The present–epoch field population includes only a very small fraction of starbursting systems (see, e.g., Zabludoff 1996), so we assume that this population can represent the universe of galaxies undergoing continuous star formation (or no star formation). Furthermore, we assume that, whatever the scatter in the relationship $\text{EW}(\text{H}\delta) = f(\text{EW}([\text{O II}]))$ for continuously star–forming galaxies, there is a well-defined mean of EW(H δ) for each EW([O II]) that does not vary significantly with epoch or environment, at least since $z = 1.0$.³ If that is so, then the expected mean values of EW([O II]) and EW(H δ) of any population depend on only two independent relations: the $\text{EW}(\text{H}\delta) = f(\text{EW}([\text{O II}]))$ relation, and the distribution of EW([O II]) values within the population.

³For young populations, $\tau < 1\text{Gyr}$, the continuum in the [O II] to H δ part of the spectrum comes from the young stars themselves, so it will not evolve with epoch. For old populations, $\tau > 5\text{Gyr}$, the continuum slope will slowly change with time, but this will be a very small effect in an era of declining SFR. Only for intermediate age populations might there be a measurable difference in the relationship of EW([O II]) and EW(H δ), but with the proximity in wavelength of these features, the effect should be second order at best.

We determine the mean $\text{EW}(\text{H}\delta) = f(\text{EW}([\text{O II}]))$ relation for continuous star-forming galaxies in two steps. Goto (2003) has determined values of $\text{EW}([\text{O II}])$ and $\text{EW}(\text{H}\delta)$ for 95,479 galaxies in the Sloan Digital Sky Survey, using line fitting methods similar to those which we have employed. These galaxies are overwhelmingly low-redshift field galaxies, and thus represent the population we wish to use. Goto’s published data on $\text{EW}(\text{H}\delta)$ have been corrected for infilling of the absorption line by emission. Our observations are of insufficient resolution and S/N to do the same, but Dr. Goto has kindly provided to us the uncorrected values, which we use. Furthermore, although Goto’s method is very similar to ours, it is not identical. To correct for systematic differences in $\text{H}\delta$ linestrengths between Goto’s and our techniques, we use the more limited measurements of $\text{EW}([\text{O II}])$ and $\text{EW}(\text{H}\delta)$ in the DS field population, to apply a shift of zero point and slope to the Goto relation. The resultant curve, which we shall take as the expected relation between $\text{EW}([\text{O II}])$ and $\text{EW}(\text{H}\delta)$ for continuously star forming galaxies in our measurement system, is presented in Figure 4.

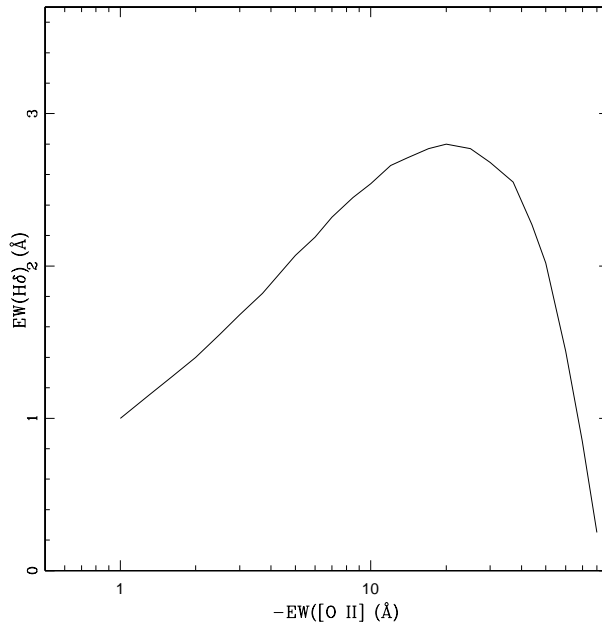


Fig. 4. Adopted relationship between mean $\text{EW}(\text{H}\delta)$ and mean $\text{EW}([\text{O II}])$ for galaxies undergoing continuous star formation.

Figure 4 shows that, due to infilling, and the fact that $\text{EW}(\text{H}\delta)$ peaks for A stars but then decreases for younger populations that include O and B stars, there is a well-bounded range of $\text{H}\delta$ strengths for continuously star-forming systems. However, this range is more than large enough to span the measurements of $\text{EW}(\text{H}\delta)$ in our composite samples of cluster

and field galaxies, as seen in Figure 2. This suggests that populations of continuously star-forming galaxies *could* reproduce most of the line strengths we observe. In fact, as we now demonstrate, they do not.

Balogh et al. (2004) have shown, using the 2dF galaxy sample, that star formation is remarkably uniform in the sense that, although the mean star formation rate (SFR) varies radically with environment, this is due almost entirely to variation in the *fraction* of star-forming galaxies. *Among only star-forming galaxies, the distribution of star formation rates is nearly independent of environment.* Wilman et al. (2004) have demonstrated the same phenomenon at $z \sim 0.4$. Indeed, even the variation of the SFR distribution of star-forming galaxies with epoch is modest: at higher redshifts it is skewed somewhat towards higher rates, but the mean $\text{EW}([\text{O II}])$ for star-forming galaxies at $z \sim 0.4$ is only about 20% higher than it is today (see Bower & Balogh 2004).

As a consequence of the small variation in the distribution of SFRs of star-forming galaxies *and* the small range in $\text{EW}(\text{H}\delta)$ with $\text{EW}([\text{O II}])$ shown in Fig. 4, the expected mean $\text{H}\delta$ strength of populations of continuously star-forming galaxies is a very stable number. We calculate that number for two cases: a low SFR case taken from the low redshift 2dF group sample, and a high SFR case taken from the $z \sim 0.4$ CNOC2 field sample. For both, we start with the observed distribution of $\text{EW}([\text{O II}])$ for star forming galaxies, from Wilman et al. (2004). In both cases we extend the distributions to weaker $\text{EW}([\text{O II}])$, from the 5 Å limits reported by Wilman et al., down to 1 Å, using the data on the LCRS sample from Hashimoto et al. (1998). For the low and high SFR samples, which have mean $\text{EW}([\text{O II}])$ of 21 Å and 28 Å, respectively, we calculate mean values of $\text{EW}(\text{H}\delta)$ of 2.8 Å and 2.6 Å, using the $\text{EW}(\text{H}\delta) = f(\text{EW}([\text{O II}]))$ relation in Figure 4. It is striking that the mean $\text{EW}(\text{H}\delta)$ is *lower* in the population with higher star-formation, because of the larger fraction of galaxies with emission infilling and the shift to younger, hotter stellar populations. For the passive, non-star-forming galaxies, we use the sum of all E galaxies in the DS sample to obtain mean a value of $\text{EW}(\text{H}\delta) = 0.9$ Å and a limit $\text{EW}([\text{O II}]) > -1.0$ Å.

With each of these two sets of mean $\text{EW}([\text{O II}])$ and $\text{EW}(\text{H}\delta)$ strengths, we can now form a one-parameter family of galaxy populations, where the parameter is the fraction of galaxies with star formation. The dashed and dotted lines of Figure 2 show the locus of points of different mixes of passive and star forming galaxies, for the low and high SFR distributions. Since the 2dF group sample and the CNOC field sample seem to span the range of $\text{EW}([\text{O II}])$ distributions, at least out to $z \sim 0.5$, the region between these two curves in Figure 2 represents the locus of possible values in this plane for populations of galaxies with (mainly) continuous star formation. It is noteworthy that — as it should be — all of the low-redshift populations, both individual clusters and mean cluster and field populations,

are consistent with this region. In other words, they are well described by mixes of passive galaxies and continuously star forming galaxies. In contrast, all higher–redshift populations lie *above*, implying that $H\delta$ is stronger than can be produced from what is today’s “normal” star formation. The straightforward conclusion is that starbursts make up a substantially greater part of the population of both cluster and field galaxies at higher redshift. This is arguably the strongest conclusion to be drawn from this paper, that neither the cluster nor field population at intermediate redshift can be made from a common mix of today’s galaxies: a much higher fraction of galaxies experiencing starbursts must be invoked.⁴

4.2. More detailed information on stellar populations from high S/N profiles of $H\delta$ absorption

With the higher signal–to–noise and higher spectral resolution now available with 6–10 meter telescopes and efficient spectrographs, it is possible to measure the strengths of individual absorption lines in the blue region of intermediate– and high–redshift cluster galaxies. For example, with Keck–LRIS spectra with a typical S/N ~ 60 per resolution element, and (rest–frame) resolution of $\sim 5 \text{ \AA}$ for Abell 851, Trager, Dressler & Faber (2004) are able to measure all of the available Lick/IDS absorption line indices (Faber et al. 1985; Worthey et al. 1994). Some of the Rose (1985; 1994) blue indices are also available (bright sky lines make some of these indices unmeasurable). Indices such as CN_2 (cf. Kelson et al. 2001), Fe4383, the G band, and Ca H+H ϵ /Ca K, and even features such as Mn and Sr II around 4050 \AA , can be used along with higher–order Balmer lines to break the age–metallicity degeneracy (cf. Trager et al., in prep.; Calwell, Rose & Concannon 2003) and even study individual abundance ratios (e.g., Trager et al. 2000a,b).

Co–adding of spectra will greatly aid these kinds of studies because it allows the collection of larger, and fainter samples in equivalent time, albeit at the loss of some specificity as galaxies of a given morphological type, absolute luminosity, location, etc. For example, we formed composite spectra of 46 E and 24 S0 galaxies in the 8–cluster Morphs sample, selected only by morphology and the absence of [O II] emission. The result, shown in Figure 5, is much stronger $H\delta$ in the S0 population than in the E population. This suggests that the S0 population, on average, has been the site of more recent star formation than the E population, consistent with the picture presented by Dressler et al. (1997) that the S0 population is growing substantially at the $z \sim 0.5$ epoch. Note that this result contradicts the conclusions of Jones, Smail, & Couch (2000) who used some of the same data used in this study to conclude that the star formation histories of elliptical and S0

⁴We cannot demonstrate from these data alone that these higher points could not be the result of simply truncated, rather than bursting, star formation. The EW($H\delta$) distributions themselves, rather than their composites, form the basis for this assertion, as discussed in P99.

galaxies were indistinguishable. Our sample, which has been carefully culled to remove galaxies with ongoing star formation, seems to show something very different. Possible differences in the two studies are the inclusion of lower redshift clusters, clusters that are more evolved dynamically, and a greater proportion of brighter galaxies in the Jones et al. study.

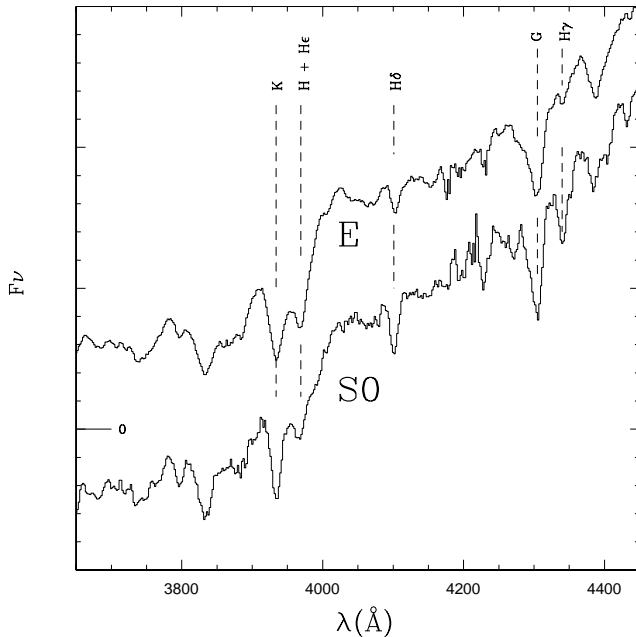


Fig. 5. The composite spectra for 46 E and 24 S0 galaxies, those in the Morphs 8-cluster sample without detectable [O II] emission $EW([O II]) \gtrsim 3\text{\AA}$. The detection of stronger H δ absorption in the S0 galaxies supports the notion that these have had more recent star formation than the elliptical galaxies.

In this paper our focus has been on the measurement of H δ with high S/N composite spectra. A careful look at its adjacent continuum reveals an epoch-dependent effect that bears on the question of how best to measure H δ in spectra of resolution 5–15 Å that is typical of studies of distant galaxies.

The higher S/N composite spectra of Figure 1 clearly show a difference in the shape of the continuum around H δ in the low-redshift cluster galaxies compared to those in the distant sample. There is a prominent peak on the blue side of the H δ line of low-redshift spectra that is not seen at higher redshift. To provide some insight into this feature, we show in Figure 6 stellar models of an aging, metal-rich stellar population from Vazdekis (1999). The models exhibit a depression of the integrated stellar continuum by the increasing prominence of CH and CN lines. The exact cause of this increase is poorly understood at present, but appears to come from the increased importance of cool giants in old, metal-rich populations (cf. Schiavon et al. 2002).

These theoretical models are in qualitative agreement with the composite data of all the

DS (low-redshift) clusters, also shown in Figure 6. It seems that, at this spectral resolution, the peak to the blue of $H\delta$ is actually a window to the true continuum, which is depressed by a blend of lines around and over $H\delta$. The models confirm, however, that $H\delta$ itself is weak, $EW(H\delta) = 1.0 \text{ \AA}$ as measured by our technique, for a 12 Gyr, solar-metal-abundance population, consistent with what we have measured. Although the models and observations roughly agree, it is apparent that this blue peak is even more prominent than predicted even by 15 Gyr-old, $[Fe/H] = +0.2$ model. The change between our 5-Gyr-old Morphs sample, for which the feature is not seen, and the present-epoch population where it is seen so clearly, indicates a more rapid evolution than the model in Figure 6 predicts. We plan in a future paper to investigate the implications of changing contamination of $H\delta$ with epoch, which is relevant not only to actually measuring line strengths but more importantly to exploit the diagnostic value of the weaker features as tracers of the stellar population history.

A final example of the information carried by the $H\delta$ line is shown in Figure 7, where we extract the $H\delta$ line for all k+a, e(a), and a+k galaxies in the Morphs sample. Comparing the spectra from k+a, e(a), and a+k shows a progression of broader (stronger) $H\delta$ with growing asymmetry. This is the signature of an earlier population of A-stars; late-B and early-A stars have Stark-broadened Balmer lines that are much stronger than even a typical A5V star. The a+k spectrum in particular appears to show a large contribution from stars as early as A0, which fixes the time of the burst to $300 \pm 100 \text{ Myr}$, while the composite k+a spectrum represents a typical age of 1 Gyr or more. This agrees with the chronology we have proposed in P99 for the population of starburst galaxies and the different spectral types we have identified (see also Barger et al. 1997).

4.3. Measuring $H\delta$ by line-fitting or bandpasses?

The two effects regarding $H\delta$ just discussed — that the continuum changes with metallicity and age, and that the $H\delta$ line becomes broad and asymmetric in young $\sim 10^8$ year-old populations — are problematical for the measurement of $H\delta$ with the commonly-used bandpass technique. As $H\delta$ grows in strength its width also increases substantially, as can be seen in Figure 5. Our line-fitting technique and bandpass measurements, using the CNOC1 definition (Balogh et al. 1999) yield nearly equivalent results between $2\text{\AA} < H\delta < 6\text{\AA}$, but begin to depart for stronger $H\delta$. For the a+k spectrum shown in Figure 7c, the bandpass method underestimates the 8.5 \AA equivalent width of $H\delta$ by 15%.

The measurement of *weak* $H\delta$ lines with the bandpass method is much more problematical. The continuum features around $H\delta$ are a function of age and metallicity, as we discuss above. This presents a problem in particular for measurements of $H\delta$ in present-epoch

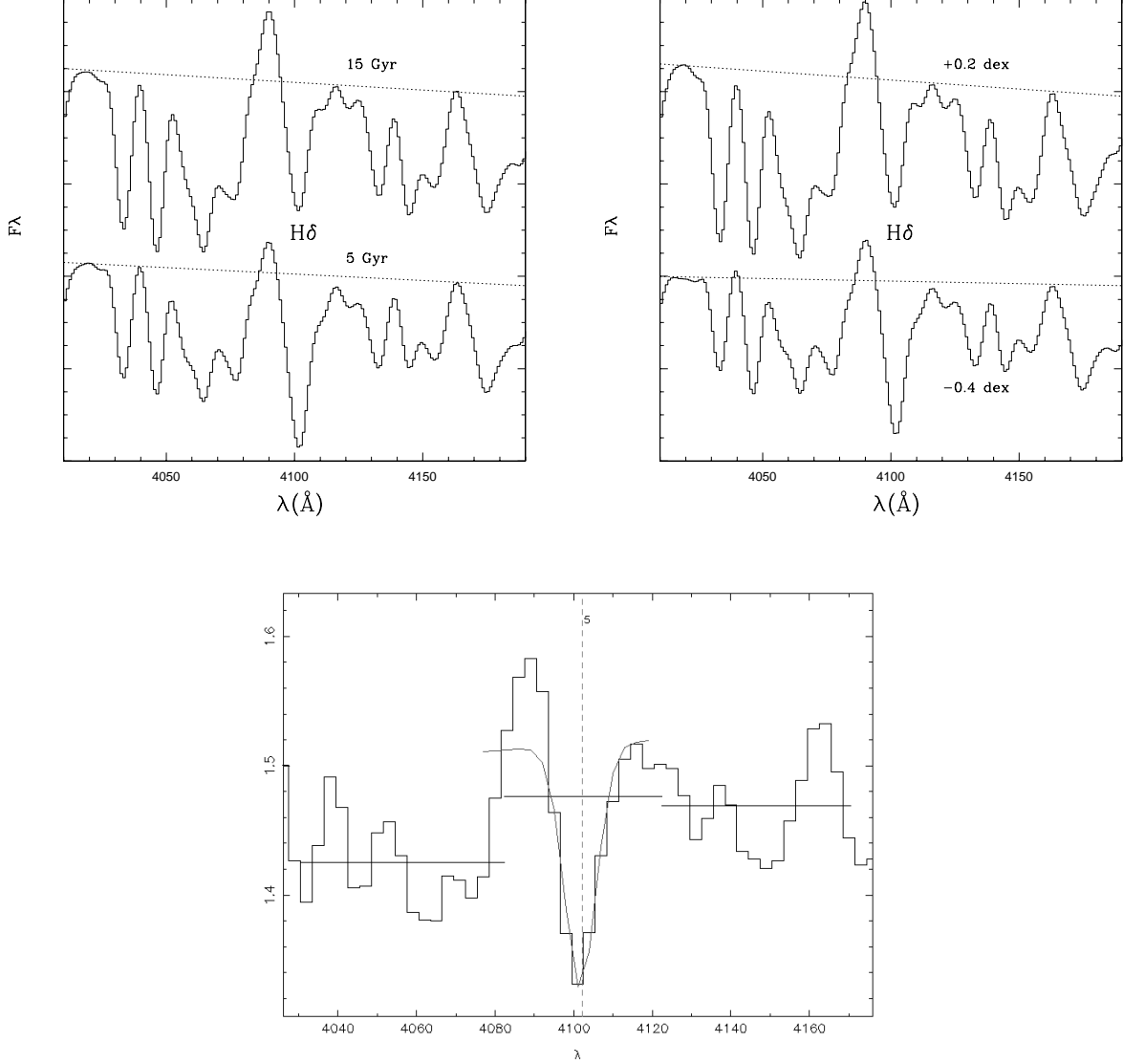


Fig. 6. Models by Vazdekis (1999) of the evolution of the integrated stellar continuum around H δ . The ordinate is in relative flux units $\text{ergs s}^{-1} \text{\AA}^{-1}$. The peak to the blue of H δ is apparently clear continuum in a growing blanket of absorption. a) (top left) the change as a stellar population ages: a 15 Gyr–old population (top) as compared to one at 5 Gyr. For models of ages 5, 8, 12, and 15 Gyr, we measure $\text{EW}(\text{H}\delta)$ of 1.4, 1.3, 1.0, and 0.9 \AA , respectively. b) (top right) a stellar population of age 12 Gyr at two different metal abundances: +0.2 dex (top) compared to –0.4 dex. For models $[\text{Fe}/\text{H}] = -0.4, +0.0, \text{ and } +0.2$ dex we measure $\text{EW}(\text{H}\delta)$ of 1.3, 1.0, and 1.0 \AA , respectively. The effect we see of larger blanketing in the H δ continuum could be the result of aging or increasing metal abundance, or both. An old and/or metal rich population has a much stronger blanketing in this region, resulting in the significant peak to the blue of H δ where the blanketing is fortuitously low. This complicates the measurement of H δ strength, particularly in old, metal-rich, stellar systems. c) (bottom) Composite spectrum of 12 DS clusters at the present epoch, showing the feature predicted in the models, at least in a qualitative sense. The line-fitting technique is able to make a sensible measurement of H δ , while the bandpass method yields a negative value, as shown by the levels marked in the figure.

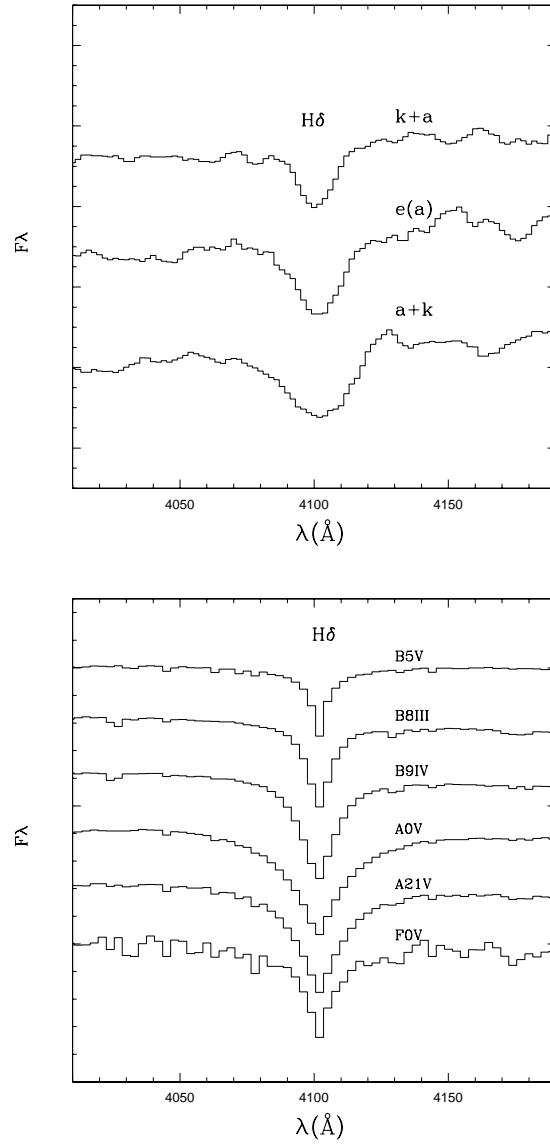


Fig. 7. Change in line profile with increasing $H\delta$ strength. a) (top), composite k+a spectra, as defined in Poggianti et al. .; b) (middle) composite e(a) spectra; c) (bottom) composite a+k spectra. The growing width and asymmetry with increasing $H\delta$ strength suggests Stark-broadened profiles of stars around type A0 in contrast to either earlier or later types. This pegs the time of the burst to 300 ± 100 Myr, while the composite k+a spectrum is typical of a burst with an age ~ 1 Gyr.

galaxies with predominantly old stellar populations. For example, the composite spectrum for all clusters in the DS sample (Fig. 1) has an $\text{EW}(\text{H}\delta) = 1.3\text{\AA}$ through the line-fitting technique, but the bandpass definition used by Balogh et al. (1999) results in a negative equivalent width (-0.8\AA) due to absorption features that depress the straddling continuum bands (see Figure 6c).

A disadvantage of the line-fitting technique the Morphs have used is that it requires relatively good spectra in order to constrain the free parameters of fitting the continuum and the line shape. The bandpass method is robust as a function of signal-to-noise, but has the problems just discussed. We conclude that, if spectra are of sufficient quality (eg., Morphs spectra quality 1–3), including of course the high S/N composite spectra used here, the line-fitting technique is preferred.

Goto (2003) has reached similar conclusions in his analysis of the SDSS spectra. That project has the additional advantage of higher spectral resolution, sufficient to resolve Balmer emission in the core of the Balmer absorption and correct accordingly. In future studies of distant galaxy populations, at least for $z < 1$, it may become common to have adequately high resolution to match the SDSS measurements with its enormous sample of galaxies, most of them at $z \lesssim 0.1$, that span such a wide array of galaxy properties.

5. Implications for the controversy over starbursts in intermediate-redshift clusters

In this study we have concentrated on measurements of [O II] emission and H δ absorption as broadly indicative of star formation histories. That galaxies in intermediate redshift clusters commonly have stronger [O II] emission, and higher rates of star formation, than do those in clusters today is an accepted fact which few dispute.⁵

On the other hand, the incidence of strong H δ absorption, and its significance for the past history of star formation in these galaxies, has been contentious. In past papers (P99, D99) we have presented data to demonstrate that 20–30% of the galaxies in the Morphs clusters have strong to very strong H δ absorption, and have argued that many, perhaps most, of these galaxies experienced a burst of star formation during their ingress to the cluster. If so, this is an essential clue to the processes which transform galaxies after they

⁵However, De Propris et al. (2003) have raised the question, based on the smaller Butcher–Oemler effect found for IR-selected samples, of whether the masses of these starforming galaxies are far below M^* (see, however, Barger et al. 1997). This issue is now under study using kinematic measurements of intermediate-redshift disk galaxies in and out of clusters.

enter clusters (see also Tran et al. 2003).

However, the observation of enhanced Balmer absorption has been questioned by the CNOC1 group (Balogh et al. 1999, hereinafter B99; Ellingson et al. 2001), who have measured [O II] and $H\delta$ strengths for 1823 galaxies in a sample of strong X-ray-emitting clusters at $0.17 < z < 0.55$ (Yee, Ellingson, and Carlberg 1996). In particular, B99 conclude that the fraction of strong Balmer-line galaxies ($EW(H\delta) > 5\text{\AA}$, $EW([O II]) < -5\text{\AA}$) is less than 5% and, in fact, consistent with *no increase* compared to the field at comparable redshift or, by comparison with the Las Campanas Redshift Survey (Zabludoff et al. 1996), no increase compared the present-epoch field. In an attempt to account for the difference, B99 questioned the (1) representative nature of the Morphs clusters, (2) the sampling of galaxies within those clusters and (3) the reality of the detections of Balmer lines.

We will return to (1) and (2) in the following section. Concerning (3), the technique of composite spectra developed in this paper allows a clear demonstration of the reality of strong $H\delta$ absorption in the Morphs clusters. An inspection of Figure 1 shows the prominence of $H\delta$ absorption (all the more remarkable since the majority of cluster galaxies, with their classical K-type spectra, have very weak Balmer lines), and the contrast with the DS sample of present-epoch clusters is striking.

However, as B99 have pointed out, relying on a single feature such as $H\delta$ can be risky in noisy data, because co-adding of features that are pure statistical fluctuations will also produce what appears to be a more certain detection. Hence, a great deal of the discussion in B99 focuses on “correcting” the CNOC1 data for the noisy measurements of $H\delta$ that are supposedly not really detections at all. That this is not the case in the Morphs data is shown in Figure 8, where we have formed composite spectra by separating the sample into groups by their *individual* measurements of $H\delta$. That $H\delta$ grows stronger group by group is, again, expected: this would happen even if we were only measuring noise. More importantly, Figure 8 shows that, as $H\delta$ increases in strength, the ratio of Ca H+H ϵ to Ca K also steadily increases, as do H γ and the higher order Balmer lines. Even for the group $1.5 < H\delta < 3.0$, below the Morphs threshold for a k+a galaxy, several of the Balmer absorption lines are seen, at their expected strengths. The obvious presence of many Balmer lines (clearly seen in Figure 8: H γ , H ϵ , and H ζ) in the composite spectra proves that the $H\delta$ absorption lines identified in the Morphs spectra are genuine.

5.1. Why the difference between CNOC1 and Morphs?

The composite spectra presented here rule out one explanation for the discrepancy between the Morphs and CNOC1 results, the suggestion by B99 that the Morphs H δ detections are spurious. Another of B99’s suggestions relates to the statement in D99 that the Morphs selection of objects for spectroscopy was based on morphology. As it turned out, despite the Morphs’s attempt to include a greater fraction of late-type galaxies (for those areas covered by the HST images), two features of the galaxy distribution — the freedom to select galaxies for a multislit mask is substantially limited by their spatial distribution, and the probability that a target galaxy is either foreground or background rises considerably with later Hubble type — conspired to minimize the difference between the Morphs selection and a pure magnitude-limited selection. The biases that resulted, discussed in P99, can be used to estimate how much more likely was it that a galaxy with strong Balmer lines (k+a, a+k, or e(a)) is included compared to a strictly magnitude limited sample. The result is that, for the area covered by the HST exposures, there is a 23% greater likelihood that one of these types will be included. When the remaining area (for which no morphological information is available was available and thus only magnitude–limited selection was used) is included drops this to well below 20%. This is probably significant, but much too small to explain the difference between the Morphs and CNOC1 studies in detecting galaxies with strong Balmer lines.

Other than this selection bias, the only differences between the data samples that we have identified is that the Morphs reach about 0.5 mag deeper ($R \sim 22.0$ at $z \sim 0.45$, the average redshift of the Morphs sample), and that the typical Morphs spectra have about twice the S/N of the typical CNOC1 spectra (by simple inspection) shown in Yee et al. (1996). Measurements of H δ in particular are sensitive to quality of the data, because of the complicated and varying continuum shape around the feature, as discussed earlier.

Apparently, then, both the Morphs and CNOC1 samples probe similar depths to similar completeness. We have shown that our detection of strong H δ absorption in $z \sim 0.5$ cluster galaxies is genuine — why has it not been seen in the CNOC1 data? An important first point is that, although the total CNOC1 sample is very large, only 4 of the clusters overlap the redshift range of the Morphs sample, $0.37 < z < 0.57$. These 4 clusters contribute only about 300 cluster members to the CNOC1 sample (see B99, Fig. 21), Also, because of a S/N cut applied by B99, not all the 300 are included in the search for k+a galaxies. The remaining sample over the relevant redshift range, though unspecified, is clearly *smaller* than the 427 cluster members of the Morphs sample.

Second, B99 chose a higher threshold of 5 Å for inclusion into the k+a category, compared to the 3 Å definition used by the Morphs, which we have just shown by Figure 8 is

supportable with the generally higher S/N Morphs spectra. This difference alone accounts for a factor of two in the fractions of k+a galaxies, since $\sim 50\%$ of the k+a/a+k galaxies in the Morphs cluster sample have $3 \text{ \AA} < H\delta < 5 \text{ \AA}$. Even with this more restrictive definition, B99 do find a fraction of 4.4% of k+a galaxies in their *entire* cluster sample, equivalent to about 9% with the Morphs definitions. There is, unfortunately, no breakdown specific to the Morphs redshift range.⁶

Third, there is a difference between the two studies of the method adopted to measure $EW(H\delta)$. We argue above that our method of measuring $H\delta$ line strengths by profile fitting is preferred over the bandpass method used by the CNOC1 group, but over the stronger $EW(H\delta) > 5.0 \text{ \AA}$ range used in CNOC1 the two techniques are in decent agreement, as B99 also conclude. However, from the discussion in Section 3.2, we note that the bandpass technique significantly underestimates the strength of $H\delta$ when $H\delta$ is weak, due to systematic changes in the continuum. Because of this, the B99 distributions of $H\delta$ strength are significantly skewed to lower $EW(H\delta)$, which leads to the derivation of a large scatter around zero $H\delta$ strength. This effect is quite evident in Fig. 28 of B99, where the CNOC1 method is seen to substantially underestimate $H\delta$ strength (applied to Morphs spectra and compared to Morphs data) for $EW(H\delta) < 5.0 \text{ \AA}$. As a result, the scatter in $H\delta$ measurements is *overestimated*, and this becomes a key factor in B99’s argument that there is no statistically significant excess of k+a galaxies in the CNOC1 clusters.

Tran et al. (2003) have reached the same conclusions regarding the CNOC1 measurements reported in B99, that there is a zero-point shift and an overestimate of the errors in $H\delta$ measurements. For their own sample of high S/N spectra in three clusters $0.33 < z < 0.83$ (one common to B99) Tran et al. find an intermediate fraction of 7–13% of ‘E+A’ (here k+a) galaxies, which they consider highly significant and indicative of a major component of galaxy evolution in clusters.

⁶Instead, Figure 22 of B99 is used to show no growth in this fraction with increasing redshift, however, this plot was made after “correcting” the counts for supposedly large errors in the CNOC1 spectral measures.

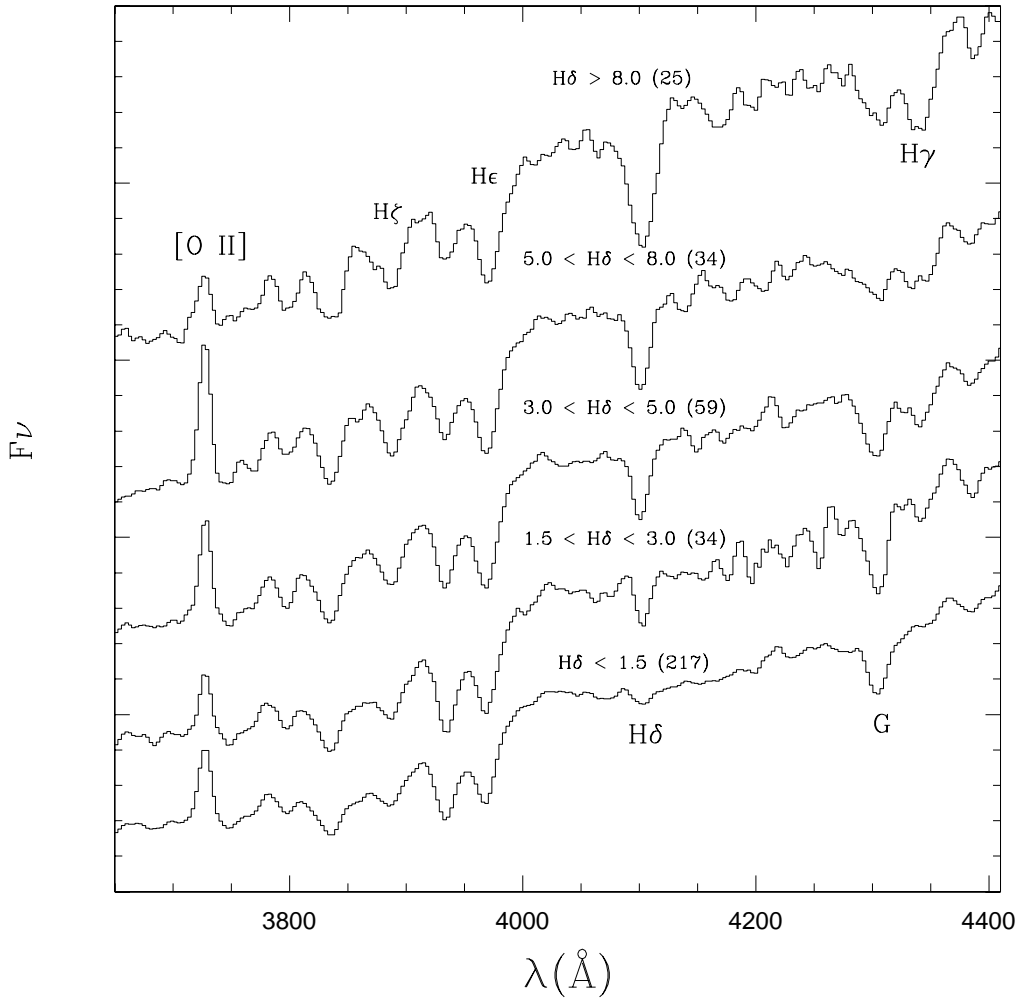


Fig. 8. Composite spectra for Morpher sample galaxies with $H\delta$ absorption recorded in 5 ranges of strength. The clear trend of increasing $H\delta$ strength and corresponding other members of the Balmer series (note, in particular, $H\gamma$, $H\epsilon$, and $H\zeta$ marked on top spectrum) shows the reality of the $H\delta$ measurement, even in the presence of substantial noise in the continuum of the spectra of individual objects.

In summary, it is not clear that a discrepancy actually exists between the Morpher finding of a significant fraction of k+a galaxies and the results from CNOC1. Differences in the quality of the data and its treatment may explain much or even all of the disagreement. If further work confirms a significantly different fraction of k+a galaxies in these two cluster samples, it could be evidence for the suggestion by Ellingson et al. (2001) that the difference in galaxy populations reflects a difference in the two cluster samples. Specifically, the X-ray-selected clusters of CNOC1 include only rich, relaxed clusters, while the Morpher clusters offer a wider diversity in properties, for example, Abell 851, a cluster with strong subclustering

that is apparently undergoing rapid dynamical evolution.⁷ If it is true that spectral evolution is correlated with cluster characteristics, this would be a very helpful clue towards identifying the mechanisms that drive the evolutionary phenomena which we observe.

Of course, a range in cluster properties could be an advantage when investigating the evolution of cluster galaxies and attempting to identify mechanisms of environmental influence. It is sensible to speculate that very luminous X-ray clusters at intermediate redshift might have few k+a galaxies because they are dynamically the most evolved clusters and further from their last major epoch of cluster/group merging. We note, however, that two very luminous X-ray clusters, CL0016+1609 and 3C295 (see P99) are present in the Morphs sample, both of which contain significant number of k+a galaxies. Because these are among the smallest samples in that study, we are reluctant to conclude that the galaxy populations of these two X-ray luminous clusters in the Morphs sample are as representative as those in the CNOC1 clusters. Adding further confusion, MS1054 — a very luminous X-ray cluster — appears to have a strong Balmer signature (see Fig. 2), but at its high redshift of $z = 0.83$ this might indeed reflect an earlier phase of the evolution of the most massive clusters. Until there are more and better data spanning a wide range of X-ray luminosity for $z \sim 0.5$ clusters, we can certainly not rule out the possibility that clusters with strong X-ray emission show the starburst phenomenon less prominently.

On the other hand, it worth noting that *all* of the Morphs intermediate-redshift clusters, as well as the DGhiz sample and MS1054, have a larger population of Balmer-strong galaxies than nearby clusters, regardless of their masses/luminosities/morphologies (Fig. 2). This suggests that cluster-to-cluster variations, at least for clusters as rich as these and over this redshift range, are a second-order factor compared to evolutionary effects — an important result on its own. The Morphs sample of 10 clusters is still too small to demonstrate this conclusively or to make a statistically meaningful test for second-order effects. Larger samples of clusters encompassing a wide range in X-ray luminosities/optical properties will be needed to assess the variation of the evolutionary trends with global cluster properties. The RCS (Gladders & Yee 2004), ACSCS, EDisCS (see www.mpa-garching.mpg.de/ediscs), and MACS (Ebeling, Edge, & Henry 2001) studies now underway will offer much-needed additional data.

⁷For comparison, the intermediate-redshift ($z > 0.35$) CNOC1 sample spans a factor of 4.4 in X-ray luminosity compared to the Morphs range of 17.

6. Summary

We have shown the utility of composite spectra for consolidating the evolution of cluster populations and significantly improving the quality of diagnostic measurements. Our choice of parameters $\text{EW}(\text{H}\delta)$ and $\text{EW}([\text{O II}])$ which separate populations of very different ages, makes it possible to dissect a cluster population by first adding the spectra of individual galaxies, thereby overcoming a principal limitation of the data.

With this technique, we have demonstrated the reality of the Morphs $\text{H}\delta$ measurements, and have shown that the line-fitting technique is the preferred method of measuring $\text{H}\delta$ over a wide range of $\text{H}\delta$ strengths, and the high S/N of these composite spectra make it a very robust technique. We have used these composite spectra to show that the clusters in our sample separate cleanly between low and higher redshift, with much stronger Balmer absorption for the latter. Although the sample is small, this result suggests that cosmic evolution has played a more important role in the evolution of cluster galaxies than has the range in cluster properties.

We have also found that field galaxies at the same redshift also appear to have stronger Balmer lines than today’s composite field galaxy populations. By comparing to a present-epoch field sample, the 2dF, we have shown that these higher redshift populations cannot be made of any mixture of passive and continuously star forming galaxies, and that starbursts must be occurring in a greater fraction of these higher redshift galaxies.

The high S/N of composite spectra enable the study of subtle features of the stellar populations of distant galaxies. The technique of producing composite spectra of cluster populations should also facilitate the construction of so-called Madau plots that trace the evolution of star formation over time. Although these have been limited to field populations, it is clear that an important step forward will be the construction of the trend of star formation over epoch *and* environment (see, for example, Postman, Lubin, & Oke 2001, Bower & Balogh 2004). As N-body simulations become better at predicting star formation along with the growth of dark-matter halos, data of this kind will put strong constraints on the models.

REFERENCES

- Balogh, M.L., Morris, S.L., Yee, H.K.C., Carlberg, R.G., & Ellingson, E., 1999, ApJ, 527, 54 (B99)
- Balogh, M.L., Eke, V.R., Miller, C., Lewis, I.J., Bower, R.G., Couch, W.J., Nichol, R., & the 2dF team, 2004, MNRAS, 348, 1353

- Barger, A. J., Aragon–Salamanca, A., Ellis, R. S., Couch, W. J., Smail, I., Sharples, R. M. 1997, MNRAS, 279, 1
- Bower, R. G., & Balogh, M. L. 2004, in *Carnegie Observatories Astrophysics Series, Vol. 3: Clusters of Galaxies: Probes of Cosmological Structure and Galaxy Evolution*, ed. J. S. Mulchaey, A. Dressler, and A. Oemler (Cambridge: Cambridge Univ. Press)
- Broadhurst, T. J., Ellis, R. S., & Shanks, T., 1988, MNRAS, 235, 827
- Butcher, H., & Oemler, A. Jr., 1978a, ApJ, 219, 18
- Butcher, H., & Oemler, A. Jr. 1978b, ApJ, 226, 559
- Caldwell, N., Rose, J. A., & Concannon, K. D. 2003, AJ, 125, 2891
- Couch, W. J., & Sharples, R. M., 1987, MNRAS, 229, 423
- De Filippis, E., Schindler, S., & Castillo–Morales, A., 2003, A&A, 404, 63
- De Propris, R., Stanford, S. A., Eisenhardt, P., & Dickinson, M. 2003. Ap&SS, 285, 43
- Dressler, A., & Shectman, S. A., 1988, AJ, 95, 284 (DS)
- Dressler, A., & Gunn, J. E., 1982, ApJ, 263, 533
- Dressler, A., & Gunn, J. E., 1983, ApJ, 270, 7
- Dressler, A., Oemler, A. Jr., Couch, W. J., Smail, I., Ellis, R. S., Barger, A., Butcher, H., Poggianti, B. M., & Sharples, R. M., 1997, ApJ, 490, 577 (D97)
- Dressler, A., Smail, I., Poggianti, B. M., Butcher, H., Couch, W. J., Ellis, R. S., & Oemler, A. Jr., 1999, ApJS, 122, 51 (D99)
- Faber, S. M., Friel, E. D., Burstein, D., Gaskell, C. M. 1985, ApJS, 57, 711
- Ebeling, H., Voges, W., Bohringer, H., Edge, A. C., Huchra, J. P., Briel, U. G., 1996, MNRAS, 281, 799
- Ebeling, H., Edge, A. C., & Henry, J. P. 2001, ApJ, 553, 668
- Ellingson, E., Lin, H., Yee, H. K. C., & Carlberg, R. G. 2001, ApJ, 547, 609
- Gladders, M. D., & Yee, H. K. C. 2004, ApJS, submitted
- Girardi, M., Giuricin, G., Mardirossian, F., Mezzetti, M., Boschin, W., 1998, ApJ, 505, 74
- Giraud, E. 1990, A&AS, 83 1
- Goto, T. 2003, PhD Thesis, University of Tokyo
- Gunn, J. E., Hoessel, J. G., and Oke, J. B., 1986, ApJ, 306, 30
- Hashimoto, Y., Oemler, A. Jr., Lin, H., & Tucker, D. L. 1998, ApJ, 499, 589
- Kauffmann, G., et al. 2003 MNRAS, 341, 33

- Kelson, D. D., van Dokkum, P. G., Franx, M., Illingworth, G. D., Fabricant, D. 1997, ApJ, 478, L13
- Kelson, D. D., Illingworth, G. D., van Dokkum, P. G., Franx, M. 2000, ApJ, 531, 184
- Kelson, D. D., Illingworth, G. D., Franx, M., & van Dokkum, P. G. 2001, ApJ, 552, L17
- Jones, L., Smail, I., and Couch, W. J., 2000, ApJ, 528, 118
- Margoniner, V. E., de Carvalho, R. R. 2000, AJ, 119, 1562
- Margoniner, V. E., de Carvalho, R. R., Gal, R. R., Djorgovski, S. G. 2001, ApJ, 548, L143
- Oemler, A. Jr., Dressler, A., Poggianti, B. M., Smail, I., Couch, W. J., & Ellis, R. S. 2004, in preparation
- Poggianti, B. M., Smail, I., Dressler, A., Couch, W. J., Barger, A. J., Butcher, H., Ellis, R. S., & Oemler, A. Jr. 1999, ApJ, 518, 576 (P99)
- Postman, M., Lubin, L. M., & Oke, J. B. 2001, AJ, 122, 1125
- Rose, J. A. 1985, AJ, 90, 1927
- Rose, J. A. 1994, AJ, 107, 206
- Schiavon, R. P., Faber, S. M., Castilho, B. V., & Rose, J. A. 2002, ApJ, 580, 850
- Smail, I., Dressler, A., Couch, W. J., Ellis, R. S., Oemler, A. Jr., Butcher, H., & Sharples, R. M. 1997, ApJS, 110, 213 (also available as VizieR On-line Data Catalog)
- Trager, S. C. 2004, in *em Carnegie Observatories Astrophysics Series, Vol. 4: Abundances from the Integrated Light of Globular Clusters and Galaxies*, ed. A. McWilliam, and M. Rauch (Cambridge: Cambridge Univ. Press)
- Trager, S. C., Faber, S. M.; Worthey, G. & González, J. J. 2000a, AJ, 119, 1645
- Trager, S. C., Faber, S. M., Worthey, G., & González, J. J., 2000b, AJ, 120, 165
- Trager, S. C., Dressler, A., & Faber, S. M. 2004, in preparation
- Tran, K.-V. H., Franx, M., Illingworth, G., Kelson, D. D., & van Dokkum, P. 2003, ApJ, 599, 865
- van Dokkum, P. G., Franx, M., Fabricant, D., Illingworth, G. D., & Kelson, D. D., 2000, ApJ, 541, 95
- Wilman, D. J., et al. 2004, in preparation
- Worthey, G., Faber, S. M.; Gonzalez, J. J., Burstein, D. 1994, ApJS, 94, 687
- Vazdekis, A. 1999, ApJ, 513, 224
- Yee, H. K. C. Ellingson, E., & Carlberg, R. G., 1996, ApJS, 102, 269

Zabludoff, A. I., Zaritsky, D., Lin, H., Tucker, D., Hashimoto, Y., Shectman, S. A., Oemler, A., & Kirshner, R. P. 1996, ApJ, 466, 104

TABLE 1
INTEGRATED SPECTRA

| sample | total N | $\langle z \rangle$ | EW([O II]) | EW(H δ) |
|---------------|---------|---------------------|------------|-----------------|
| Abell 548 | 100 | 0.040 | -2.9 | 1.2 |
| Abell 754 | 81 | 0.054 | > -1.0 | 0.6 |
| Abell 1631 | 71 | 0.053 | -1.8 | 1.1 |
| Abell 1644 | 90 | 0.049 | -4.1 | 1.5 |
| Abell 1736 | 96 | 0.041 | > -1.0 | 1.0 |
| Abell 1983 | 68 | 0.045 | -3.5 | 1.5 |
| Abell 2151 | 41 | 0.037 | -4.6 | 1.4 |
| DC0003-50 | 28 | 0.035 | -3.5 | 0.9 |
| DC0428-53 | 79 | 0.041 | -1.6 | 1.2 |
| DC0559-40 | 75 | 0.049 | -1.5 | 1.1 |
| DC0608-33 | 13 | 0.035 | -7.9 | 1.3 |
| DC2048-52 | 84 | 0.046 | -1.7 | 1.0 |
| DSclusters | 826 | 0.044 | -3.0 | 1.1 |
| DSfield | 130 | 0.044 | -8.4 | 1.6 |
| DS_Ellip | 161 | 0.044 | > -1.0 | 0.9 |
| A370 | 40 | 0.374 | -3.9 | 1.8 |
| CL3C295 | 18 | 0.459 | -3.7 | 2.7 |
| CL0016 | 24 | 0.546 | -4.2 | 2.4 |
| CL0024 | 97 | 0.393 | -8.3 | 1.8 |
| CL0303 | 44 | 0.418 | -9.4 | 1.8 |
| CL0939 (A851) | 84 | 0.406 | -5.4 | 2.0 |
| CL1447 | 21 | 0.376 | -9.7 | 2.3 |
| CL1601 | 51 | 0.539 | -2.3 | 2.0 |
| Morphs | 379 | 0.442 | -6.2 | 2.0 |
| Morphs field | 50 | 0.450 | -14.1 | 2.7 |
| Morphs k | 150 | 0.450 | > -1.0 | 1.2 |
| DGhiz | 60 | 0.748 | -7.4 | 2.0 |
| MS1054 | 72 | 0.803 | -4.1 | 2.3 |
| DGhizfield | 25 | 0.750 | -27.2 | 3.7 |
| DGintzfield | 23 | 0.450 | -24.8 | 3.4 |